A | R | J
Amrit Research Journal December 2024, Vol. 5, Issue 1, 140-150
ISSN: 2738-9553
RESEARCH ARTICLE

A Computational DFT Insight into the Optimized Structure, Electronic Structures, Spectroscopic Analysis, and Thermodynamic Parameters of the Cytosine Molecule

Khakendra Basnet[1], Bhijan Neupane[1], Pima Gharti Magar[1], Roshika Uprety[1], Krishna Bahadur Rai[1*]
[1]Department of Physics, Patan Multiple Campus, Lalitpur, Tribhuvan University, Nepal
[*]Email: krishnarai135@gmail.com
(Received: July 5, 2024; Received in Revised form: September 9, 2024; Accepted: September 12, 2024; Available online)

DOI: https://doi.org/10.3126/arj.v5i1.73566

Highlights

- The Cytosine molecule and its optimized structure was obtained using density functional theory (DFT) at the B3LYP/6-311++G(d,p) basis set.
- An energy gap obtained from the density of states was 4.92 eV and this clarified to equivalent orbital energy gap levels.
- The vibrational of C-H, N-H and C=O were found to be in the range of 3100-3300 cm^{-1} 3500-3700 cm^{-1} and, 1771.10 cm^{-1} respectively.
- Thermodynamic properties such as heat capacity, internal energy, enthalpy and entropy increase with increase in temperature while Gibbs free energy shows opposite trend.

Abstract

The optimized structure of the Cytosine molecule was achieved in 12 steps, yielding an optimization energy of -10749.84 eV. The HOMO-LUMO energy gap of 4.94 eV indicates chemical stability. The oxygen atom exhibits the most negative potential and the hydrogen atom shows the most positive potential. The density of states reveals an energy gap of 4.92 eV, confirming equivalent orbital energy levels. Calculated hardness (2.47 eV) and softness (0.41 eV^{-1}) suggest stability and polarizability. The chemical potential is -3.97 eV, and the electronegativity is 3.97 eV. The electrophilicity index of 3.19 eV indicates a strong electrophilic behavior. Mulliken charge analysis identifies H13 with the highest positive charge and N5 with the highest negative charge. Vibrational analysis shows C-H vibrations at 3100-3300 cm^{-1}, N-H at 3500-3700 cm^{-1}, and C=O at 1771.10 cm^{-1}. Thermodynamic properties such as heat capacity, internal energy, enthalpy, and entropy increase with temperature, while Gibbs free energy decreases.

Keywords: *Density Functional Theory, HOMO-LUMO gap, Mulliken charges, Vibrational analysis, Thermodynamic properties*

Introduction

Cytosine (molecular formula $C_4H_5N_3O$) is a crucial building block in Deoxyribonucleic acid (DNA) and Ribonucleic acid (RNA) which make up their genetic codes [1]. It has a specific structure with a ring and certain groups at different positions. Cytosine, along with two other bases (i.e. uracil and thymine) form the pyrimidine family which has a single-ring structure. This unique structure allows the title molecule to pair up with another specific base guanine by creating a stable pair in the DNA and RNA structures. Beyond this pairing role, the title molecule can undergoes changes that affect how genes work [2]. It can influence

[*]*Corresponding author*

various aspects of an organism's life like development and disease susceptibility. Additionally, the title molecule can team up with phosphate groups to become Cytidine triphosphate (CTP), an energy carrier in the cell that helps with different biochemical processes [3]. So, cytosine plays multiple important roles in the working machinery of DNA.

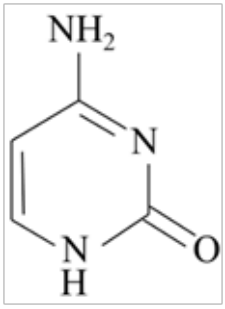

Fig 1. Chemical structure of Cytosine ($C_4H_5N_3O$) molecule

Fig. 1 shows the molecular structure of Cytosine ($C_4H_5N_3O$) molecule having sum of 13 bonds. It includes 8 bonds excluding hydrogen (non-H), 3 bonds with multiple connections, 3 double bonds, 1 six-membered ring, 1 aliphatic imine, and 1 aliphatic primary amine. Density Functional Theory (DFT), an essential tool assists as the best platform for quantum computations and molecular modeling [4-6]. Recognized for its adaptability and precision, researcher uses a range of theoretical methods and basis sets to forecast molecular structures of geometry optimization, energetics, and spectroscopic characteristics (frequency analysis) across various domains which include organic, inorganic, and biochemistry, as well as materials science and drug discovery [7-10]. Gaussian's applications extend to investigating properties like geometries, energies, transition states, and reaction mechanisms [11]. Notable studies include DFT investigation over similar title molecule's catalyzing double-proton transfer with guanine [12] as well as surface studies on gallium- and aluminum-doped graphene and their impact on the title molecule's absorption [13, 14, 15]. The various study dives into molecular electrostatic potential analysis using various approaches [16] and explores their vibrational studies of the molecule and related compounds [17]. Additionally, it covers electrostatic potential analysis [18] and electron density alpha, beta and spin density studies [19].

Despite these works, there are still lacking on the systematic study on the optimized molecular structure, electronic structures, vibrational analysis, thermodynamic properties and their interpretations through the quantum mechanical treatments. Therefore, this work attempts to investigate molecular optimized molecular structure, highest occupied molecular orbitals and lowest unoccupied molecular orbital (HOMO-LUMO) analysis, molecular electrostatic potential (MEP), electrostatic potential (ESP), electron density (ED), density of states (DOS), global reactivity descriptors, Mulliken charges, vibrational analysis and thermodynamic properties using the DFT/B3LYP method and 6-311G basis set, a balanced and cost-effective approach.

Computational Methodology

Gaussian's software products are proven as a powerful and widely accepted computational tool for studying molecular properties. All quantum chemical calculations for the $C_4H_5N_3O$ molecule was conducted using the Gaussian09W program [11]. GaussView 6.0 [20] was used for both analyzing and visualizing the molecular results. Initially, the DFT/B3LYP approach was used to optimize the shape of the chosen molecule using the 6-311++G(d, p) basis set. The vibrational behavior (wavenumbers) was then calculated using these optimized structural parameters. Using the same basis set, the DFT approach was used to compute the molecule's electrostatic potential, electrostatic potential, Global Reactivity Descriptors and the energies of its highest occupied and lowest unoccupied molecular orbitals (HOMO-LUMO). The GaussSum 3.0 program [21] was used to analyze the DOS spectrum. Additionally, thermodynamic properties were obtained using Moltran software [22], and the graphs were designed with OriginPro9.0 software.

The ionization potential (I) and electron affinity (A) are directly correlated with the HOMO and LUMO energies respectively. The amount of energy required to extract an electron from a gaseous atom is known as the ionization energy (I). Comparably, the energy released when an additional electron is added to an atom is measured by electron affinity (A). The relationship between electron affinity (A) and ionization potential (I).

Ionization Potential (I) = $-E_{HOMO}$ …… (1)

Electron Affinity (A) = $-E_{LUMO}$ …… (2)

The HOMO-LUMO energy gap is a key parameter in understanding the electronic properties of a molecule. E_{LUMO} represents the energy of the lowest unoccupied molecular orbital and E_{HOMO} represents the energy of the highest occupied molecular orbital such that Energy gap ($\Delta E = E_{gap}$) represents the HOMO-LUMO energy gap [23] i.e.

Energy gap (ΔE) = $E_{LUMO} - E_{HOMO}$ ……..…..... (3)

The formulae required for the calculation of Global Reactivity Index (GRI) parameters, Chemical hardness (η), Softness (S), Chemical potential (μ), Electronegativity (χ), Electrophilicity index (ω) [23] are presented as the following equations

$\eta = (I–A)/2$ ……..... (4)

$S = 1/\eta$ ..……..... (5)

$\mu = -(I+A)/2$ ..……..... (6)

$\chi = (I+A)/2$ ..……..... (7)

$\omega = \mu^2/2\eta$ ..……..... (8)

Results and Discussion

Optimized Structure of Cytosine's Molecule

Fig. 2(a) shows the optimized structure of Cytosine molecule and it is a heterocyclic molecule characterized by a ring structure containing two nitrogen atoms. Optimization refers to the process of determining the most stable molecular geometry of the molecule under specific conditions. In the study of cytosine, the molecule is optimized in 12 steps, and the Hartree energy versus optimization step number is plotted in fig. 2(b). The graph indicates that the optimization process stabilized after the 12th step. As can be seen in fig. 2(b) the molecule has finally reached step number 12, where its energy has been lowered to the lowest possible energy state and has remained stable at this point with an energy of -10749.84 eV (-395.04192 Hartree).

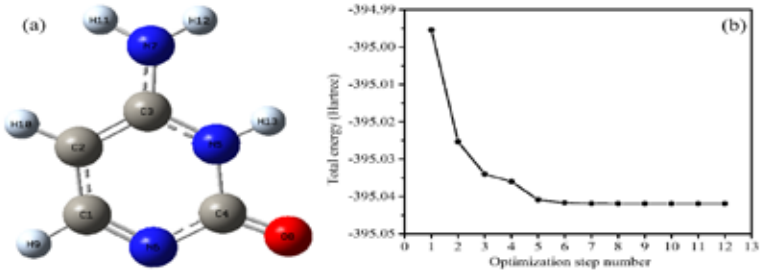

Fig. 2. (a) Optimized molecular structure of cytosine and (b) Plot for total energy vs optimization step number of title molecule

Based on Gaussian calculations, the title molecule exhibits bond lengths, bond angles, and dihedral angles, as detailed in Table 1. The bond lengths and bond angles are consistently positive, while dihedral angles encompass both positive and negative values [24]. A bond length represents the distance between two connected atoms, a bond angle involves three connected atoms, and a dihedral angle pertains to four connected atoms. These geometric parameters provide essential details about the molecular structure and configuration of the title molecule. The positive and negative values in dihedral angles indicate the molecular conformation by contributing to a detailed understanding of the title molecule's geometry.

Table 1. Calculated values of bond length (Å), bond angle (°) and dihedral angle (°) of Cytosine molecule

Atoms	Bond Length (Å)	Atoms	Bond Angle (°)	Atoms	Dihedral Angles (°)
C(1)–C(2)	1.4081	C(1)-C(2)-C(3)	116.5904	O(8)-C(4)-N(5)-H(13)	-2.2271
C(1)-N(6)	1.3145	C(2)-C(3)-N(5)	117.3183	H(13)-N(5)-C(3)-N(7)	0.3551
C(2)-C(3)	1.3824	C(3)-N(5)-C(4)	124.8184	N(5)-C(3)-N(7)-H(12)	22.8858
C(4)-N(6)	1.3732	N(5)-C(4)-N(6)	116.1283	H(12)-N(7)-C(3)-C(2)	-159.3571
C(4)-N(5)	1.4365	C(4)-N(6)-C(1)	118.4594	H(11)-N(7)-C(3)-C(2)	-13.8241
C(3)-N(7)	1.3682	N(5)-C(1)-C(2)	126.6832	N(7)-C(3)-C(2)-H(10)	2.4619
C(3)-N(5)	1.3561	N(6)-C(4)-O(8)	126.6360	C(3)-C(2)-C(1)-H(9)	179.9815
C(1)-H(9)	1.0891	O(8)-C(4)-N(5)	117.5207	H(10)-C(2)-C(1)-H(9)	0.0698
C(2)-H(10)	1.0804	C(4)-N(5)-H(13)	114.0604	C(2)-C(1)-N(6)-C(4)	0.3443
C(4)-O(8)	1.2141	H(13)-N(5)-C(3)	121.0676	C(1)-N(6)-C(4)-O(8)	179.6307
N(5)-H(13)	1.0121	N(5)-C(3)-N(7)	117.9964	N(6)-C(4)-N(5)-C(3)	0.3994
N(7)-H(11)	1.0076	H(11)-N(7)-H(12)	114.9095		
N(7)-H(12)	1.0085	H(11)-N(7)-C(3)	117.1238		
		N(7)-C(3)-C(2)	124.6495		
		C(3)-C(2)-H(10)	121.5360		
		H(10)-C(2)-C(1)	121.8735		
		C(2)-C(1)-H(9)	117.9083		
		H(9)-C(1)-N(6)	115.5479		

Electronic Structures

HOMO and LUMO analysis

Analyzing HOMO and LUMO calculations is crucial for understanding the title molecule's electronic characteristics. The HOMO denotes the highest occupied electron energy level, while the LUMO denotes the lowest unoccupied energy level. A smaller energy gap between HOMO and LUMO suggests a higher likelihood of electronic transitions and vice versa [25]. This gap gives a valuable information about the molecule's reactivity, stability, and propensity for electronic transitions. Fig. 3 displays the Cytosine molecule's HOMO-LUMO plot and frontier orbital energy gap. The energy differences between HOMO and LUMO is 4.94 eV (in neutral state), with HOMO's energy being -6.44 eV and LUMO's energy being -1.50 eV. The negative LUMO energy signifies the ability of the molecule to accept electrons to further contribute to its reactivity [26]. In this Cytosine molecule, the energy gap indicates that the molecule is stable one.

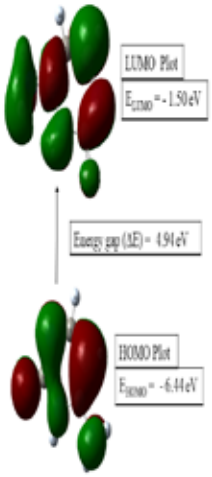

Fig. 3. HOMO and LUMO orbitals of Cytosine

Molecular Electrostatic Potential (MEP) Analysis, Electrostatic Potential (ESP) Analysis and Electron Density(ED)

Fig. 4(a) represents visual mapping analysis of molecular electrostatic potential on its surface of Cytosine in the gas phase. High negative potential regions indicate nucleophilic attack sites, while high positive potential regions signify electrophilic attack sites. Fig. 4(a) reveals distinctive MEP distribution values with respect to the color scale, ranging from negative (red) with -8.042e-2 a.u. to positive (blue) with 8.042e-2 a.u. and these assist in recognizing reactive sites. This fig. 4(a) illustrates a notable negative potential around the oxygen and a positive potential near Hydrogen atoms and offers the details of the molecule's reactivity [17]. Fig. 4(b) shows the visual displayed electrostatic potential around the molecule by revealing its charge distribution and reactivity insights. The electrostatic potential analysis at various spatial points identifies the electrophilic and nucleophilic regions. The electrostatic potential mapped on the isodensity surface ranged from -1.592e-2 a.u. (red) to 1.592e-2 a.u. (blue) assists in understanding molecular behavior and identifying potential reaction sites for electrophilic and nucleophilic attacks. Its result contributes to predicting molecular interactions and guiding reaction design [18, 27]. The result, depicted from fig. 4(b) shows specific sites with high positive potential, indicating electrophilic reactivity and regions with high negative potential, suggesting of nucleophilic reactivity. Electron density governs properties like electrical conductivity, magnetism, and optics, influencing electronic band structure. Quantum methods like DFT compute electron density to predict and design materials with specific electronic traits [28]. Fig. 4(c) shows the electron density distribution and gives us an idea for indicating the probability of an electron to be present at a specific location.

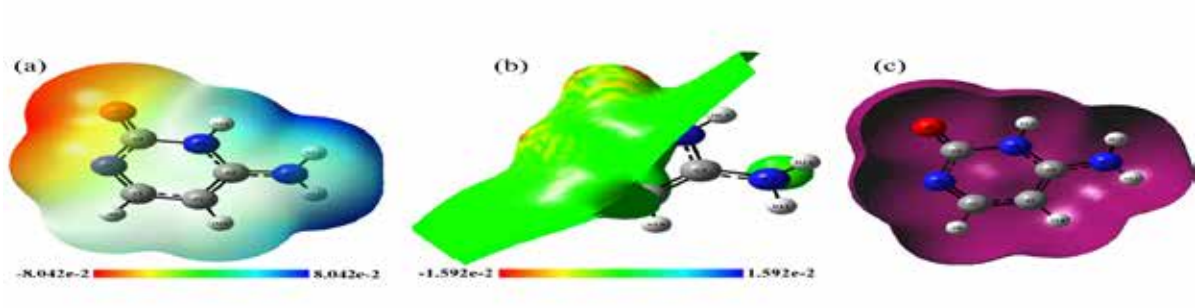

Fig. 4. (a) Molecular electrostatic potential, (b) electrostatic potential map (c) electron density of Cytocine molecule

Density of States (DOS)

The DOS spectrum provides valuable information about the density of states of a material which is crucial for understanding its electronic properties. It shows the distribution of electronic states as a function of energy. The DOS spectrum provides insights into the electronic structure, band gaps, electronic transitions and the nature of the electronic states in a material [12]. The spectral graph illustrating the DOS for the molecule is displayed in fig. 5. The distribution of the molecule's accessible electron energy levels is shown in this graph. DOS affects the probability of electron occupation by showing the number of electron states per energy level [29]. Negative DOS intensity signifies unoccupied or unstable states, whereas positive intensity denotes occupied states. Fig. 5 gives the calculated energy gap of 4.92 eV in the DOS spectrum which is closely aligned with our previously determined HOMO-LUMO energy gap, reinforcing the accuracy of our findings. GaussSum v.3.0 software was used to plot the graph, with parameters set to start at -20 eV, terminate at 0 eV, and full width at half maximum (FWHM) at 0.3 eV. An intense peak at -13.5 to -10 eV shows that electrons are filling orbitals or the valence band. Another peak that is closer to 0 eV is indicative of virtual or vacant orbitals that are open to electron transitions and may be associated with excitation or conduction band states [20, 30,]. DOS with positive values in the graph indicate a bonding interaction between orbitals, whereas negative values indicate an anti-bonding interaction. When the DOS value is 0, non-bonding interactions are indicated [31, 32].

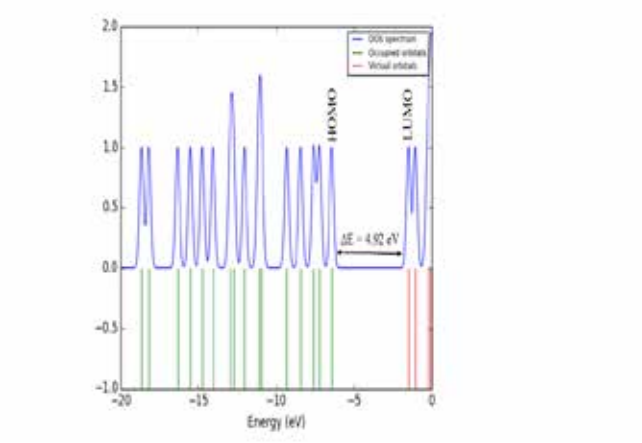

Fig. 5. DOS spectra of Cytosine molecule

Global Reactivity Descriptors

The global response descriptors are determined by evaluated energy values of HOMO and LUMO. The calculated global hardness (η) of Cytosine molecule is 2.47 eV and it indicates the molecule's stability and resistance to change or deform their lowest or the occupied orbital state which can also be called its electronic configuration due to chemical reaction [33, 34]. The inverse of the hardness is softness (S) and its value is 0.41 eV^{-1}. It means its polarizability and ease of electron transfer or ability of a molecule to donate or take electrons with ease. Chemical potential (μ) is a measure of a substance's potential energy. A molecule that has a higher negative chemical potential is more likely to react or release energy and its value is -3.97 eV. The molecule's capacity to attract electrons is indicated by its electronegativity (χ), which is 3.97 eV on calculation. The great tendency to attract electrons is shown by the higher and positive value obtained. The tendency of an atom or molecule to take an electron in a chemical reaction is indicated by the global electrophilicity index (ω), which has a value of 3.19 eV and helps anticipate how reactive a substance will be toward nucleophiles in chemical processes. The electrophilicity index (ω) is classified as strong if it is greater than 1.5 eV, moderate if it is in between 0.8 and 1.5 eV, and marginal if it is less than 0.8 eV [35, 36].

Mulliken Charges and Chemical Reactivity

Mulliken charges offer valuable insights into the molecule's polarity, influencing its reactivity and interactions across various molecular contexts [16]. Mulliken charges for the Cytosine molecule reveal distinct charge distributions on its atoms. Fig. 6 illustrates atom's charge distribution. The atoms on the Cytosine molecule exhibit positive charges in C2, C4, H9, H10, H11, H12 and H13 whereas the negative charges are displayed on C1, C3, N5, N6, N7 and O8. The atoms with the highest positive and negative charges, are H13 and N5 respectively. Positive charges on C2, C4, H9, H10, H11, H12 and H13 atoms suggest potential electron loss, indicating electrophilic regions.

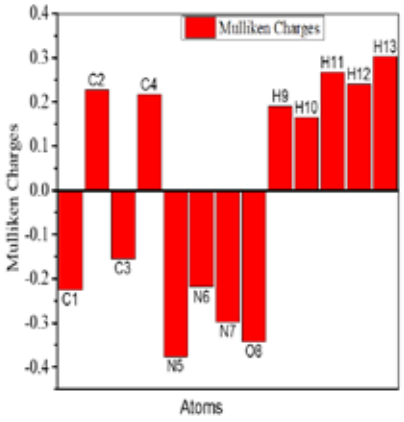

Fig. 6. Mulliken charges distribution of atoms on the Cytosine molecule

Vibrational Analysis

In the FT-IR spectra of the title molecule, specific vibrational bands are observed in the range of 4000 to 0 cm^{-1} which corresponds to functional groups such as NH_2 stretching, C=O stretching, N-H stretching, and C-H stretching vibrations [37]. FT-IR spectroscopy in fig. 7 reveals cytosine's molecular details and predicts vibrational spectra. Transmission values in IR spectra correlate with sample absorbance, quantifying radiation absorption. DFT-calculated IR spectra predict absorbance, offering insights into molecular vibrational modes and chemical bonds, with experimental validation essential for accuracy [38, 39].

C – H vibration

Because of aromatic C–H stretching vibrations, aromatic compounds show several weak bands in the 3300–3000 cm^{-1} range [26, 27]. The C-H stretching vibrations in our molecule are found at 3123.52 cm^{-1} and 3216.57 cm^{-1}.

N – H vibration

The frequency range of the N-H stretching vibrations is always in between 3500 and 3000 cm^{-1} [26, 27]. The FT-IR bands for N-H vibrations are found in 3585.63 cm^{-1}, 3588.93 cm^{-1}, and 3696.68 cm^{-1}.

C = O vibration

This stretching mode is one of the strongest peak in the absorbance band range for IR intensity associated with the carbonyl (C=O), which normally lies between 1750 and 1650 cm^{-1} [26, 27]. In our study, the C=O vibration occurs in region of 1771.10 cm^{-1}.

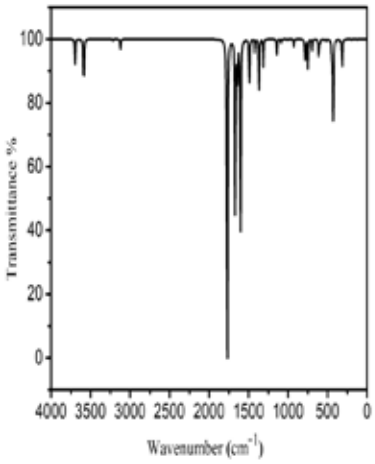

Fig. 7. IR spectroscopy for Cytosine molecule

Thermodynamic Properties

Thermodynamic properties of the Cytosine molecule involves studying the molecule's thermodynamic behavior like heat capacity at constant volume (C_v), heat capacity at constant pressure (C_p), internal energy (U), enthalpy (H), entropy (S) and Gibbs free energy (G) at various temperature. Heat capacity reveals the substance's thermal behavior, while Gibbs free energy denotes stability and reactivity under diverse conditions. Internal energy accounts for the system's total energy, and entropy reflects its disorder [40, 41]. Fig. 8 shows the graph of correlation of heat capacity at constant volume (C_v), heat capacity at constant pressure (C_p), internal energy (U), enthalpy (H), entropy (S) and Gibbs free energy (G) with the increase temperature and their polynomial fittings. Increasing rate of these thermodynamic parameters are gradual with the rise in temperature except the Gibbs free energy. The correlation equations among C_v, C_p, U, H, S and G with temperature have been fitted by quadratic (polynomial) form and the corresponding fitting factors (R^2) for C_v, C_p, U, H, S and G are equal to 0.99421, 0.99421, 0.99994, 0.99995, 0.98532 and 0.99996 respectively. The corresponding fitting equations for C_v, C_p, U, H, S and G are:

$$C_v = 15.9718 + 0.2972T + 5.0410 \times 10^{-6} T^2$$

$$C_p = 24.2871 + 0.2971T + 5.0510 \times 10^{-6} T^2$$

$$U = 256.6858 + 0.0119T + 1.5715 \times 10^{-4} T^2$$

$H = 256.68579 + 0.0202T + 1.5714x10^{-4}T^2$

$S = 181.38517 + 0.6802T – 4.5911x10^{-4}T^2$

$G = 257.81644 – 0.2126T - 2.0792x10^{-4}T^2$

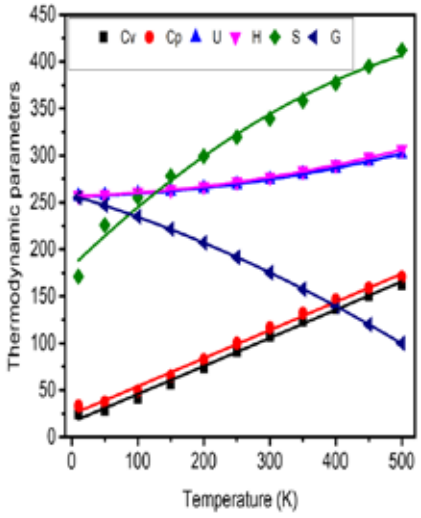

Fig. 8. Correlation plot of heat capacity at constant volume (C_V), heat capacity at constant pressure (C_p), internal energy (U), enthalpy (H, entropy (S), and Gibbs free energy (G) with temperature

Conclusions

In this study we found molecular geometry, electronic structures, global reactivity parameter, density of states, Mulliken charges, ESP, MEP, ED, vibrational analysis and thermodynamic properties of Cytosin using density functional theory (DFT) at the B3LYP/6-311++G(d, p) basis set. The optimization of the Cytosin molecule occured in twelve steps. We calculated bond length, bond angle and dihedral angle in which the highest bond length was 1.4365 Å in between C4-N5 together with the highest value for bond angle and the highest value for dihedral angle were 126.6832 degree, 179.9815 degree for N5-C1-C2, C3-C2-C1-H9 respectively. The frontier orbitals i.e. HOMO-LUMO was studied and their energy gap was found to be 4.94 eV and about equal to the energy gap i.e. 4.92 eV obtained from the density of states. The electrophilic and nucleophilic reaction sites of molecule have been predicted by ESP and MEP surface in which oxygen atom has the most negative potential indicating neucleophilic site while hydrogen atom has the most positive potential indicating electrophilic site. Similarly, the global reactivity descriptor such as chemical potential (μ), electronegativity (χ), hardness (η), softness(S), and elecrophilicity index (ω) for the cytosine molecule were found to be -3.97 eV, 3.97 eV, 2.47 eV, 0.41 eV^{-1} and 3.19 eV respectively. Mulliken charge analysis suggested that H13 has highest positive charge while N5 has the highest negative charge. The vibrational analysis has been performed in which C-H vibration was found to be in 3123.52 cm^{-1} and 3216.57 cm^{-1}. In addition, N-H vibration was found in 3585.63 cm^{-1}, 3696.68 cm^{-1} and 3588.93 cm^{-1} and C=O vibration was observed in 1771.10 cm^{-1}. Thermodynamic parameters like heat capacity, internal energy, enthalpy, and entropy increase with the increase in temperature whereas Gibbs free energy exhibits an inverse relationship with the rise in temperature.

References

1. Y.S. Chuan. Theoretical Studies of Bioferroelectricity in DNA/RNA Nucleobases and their Base Pairs. Doctoral dissertation, University of Malaya Malaysia. 2019
2. O. Doluca, J.M. Withers, V.V Filichev. Molecular engineering of guanine-rich sequences: Z-DNA, DNA triplexes, and G-quadruplexes, Chemical reviews, 2013, 113 (5), 3044-3083. (DOI: https://doi.org/10.1021/cr300225q)

3. S. Darekar, S. Laín. Asymmetric inheritance of cytoophidia could contribute to determine cell fate and plasticity. BioEssays, 2022, 44(12), 2200128. (DOI: https://doi.org/10.1002/bies.202200128)

4. P. Gharti Magar, R. Uprety, K.B. Rai. First-principles DFT study of the molecular structure, spectroscopic analysis, electronic structures, and thermodynamic properties of ascorbic acid. Himalayan Physics, 2024, 11, 28-40. (DOI: https://doi.org/10.3126/hp.v11i1.65329)

5. H.R.K. Gauli, K.B. Rai, K. Giri, R. Neupane. Monte-Carlo simulation of phase transition in 2d and 3d Ising model, Scientific World, 2023, 16(16), 12-20. (DOI: https://doi.org/10.3126/sw.v16i16.56744)

6. C.P. Dhakal, K.B. Rai. Simulating and Analyzing the Electronic Structure of a Spherical Amorphous SiO2 Nanoparticle of Finite Radius, Journal of Nepal Physical Society, 2023, 9(2), 14–22. (DOI: https://doi.org/10.3126/jnphyssoc.v9i2.62285)

7. S. Gatfaoui, N. Issaoui, A. Mezni, F. Bardak, T. Roisnel, A. Atac, H. Marouani. Synthesis, structural and spectroscopic features, and investigation of bioactive nature of a novel organic-inorganic hybrid material 1H-1,2,4-triazole-4-ium trioxonitrate, Journal of Molecular Structure, 2017, 1150, 242-257. (DOI: https://doi.org/10.1016/j.molstruc.2017.08.092)

8. O. Noureddine, S. Gatfaoui, S.A. Brandan, A. Sagaama, H. Marouani, N. Issaoui. Experimental and DFT studies on the molecular structure, spectroscopic properties, and molecular docking of 4-phenylpiperazine-1-ium dihydrogen phosphate, Journal of Molecular Structure, 2020, 1207: 27762. (DOI: https://doi.org/10.1016/j.molstruc.2020.127762)

9. P. Alivisatos, P.F. Barbara, A.W. Castleman, J. Chang, D.A. Dixon, M.L. Klein, G.L. McLendon, J.S. Miller, M.A. Ratner, P.J. Rossky. From Molecules to Materials: Current Trends and Future Directions, Advanced Materials, 1998, 10(16) 1297-1336. (DOI: https://doi.org/10.1002/(SICI)1521-4095(199811)10:16<1297::AID-ADMA1297>3.0.CO;2-7)

10. N.B.D. Lima, G.B. Rocha, R.O. Freirec, A.M. Simas. RM1 Semiempirical Model: Chemistry, Pharmaceutical Research, Molecular Biology and Materials Science. Journal of Brazilian. Chemical Society, 2019, 30(4), 683-716. (DOI: https://doi.org/10.21577/0103-5053.20180239)

11. M.J. Frisch, G.W. Trucks, H.B. Schlegel, G.E. Scuseria, M.A. Robb, J.R. Cheeseman, Jr. Montgomery, et al. Gaussian 03, revision C, 2009.

12. J. Xue, X. Guo, X. Wang, Y. Xiao. Density functional theory studies on cytosine analogues for inducing double-proton transfer with guanine, Science Report, 2020,10(1), 9671. (DOI: https://doi.org/10.1038/s41598-020-66530-8)

13. A.S. Rad, D. Zareyee, M. Peyravi, M. Jahanshahi. Surface study of gallium-and aluminum-doped graphenes upon adsorption of cytosine: DFT calculations, Applied Surface Science, 2016, 390, 444-451. (DOI: https://doi.org/10.1016/j.apsusc.2016.08.065)

14. K.B. Rai, I. B Khadka, E.H. Kim, S.J. Ahn, H.W. Kim, J.R. Ahn. Influence of hydrophobicity on the chemical treatments of graphene, Journal of the Korean Physical Society, 2018, 72(1), 107-110 (DOI: https://doi.org/10.3938/jkps.72.107.

15. S.J. Ahn, H.W. Kim, I.B. Khadka, K.B. Rai, J.R. Ahn. Electronic Structure of Graphene Grown on a Hydrogen-terminated Ge (110) Wafer, Journal of Korean Physical Society, 2018, 73(5), 656-660. (DOI: https://doi.org/10.3938/jkps.73.656)

16. M. Kohagen, F. Uhlig, J. Smiatek. On the nature of ion-stabilized cytosine pairs in DNA i-motifs: The importance of charge transfer processes. International Journal of Quantum Chemistry, 2019, 119(14), e25933. (DOI: https://doi.org/10.1002/qua.25933)

17. Z. Demircioğlu, G. Kaştaş, C.A. Kaştaş, R. Frank. Spectroscopic, XRD, Hirshfeld surface and DFT approach (chemical activity, ECT, NBO, FFA, NLO, MEP, NPA& MPA) of (E)-4-bromo-2-[(4-bromophenylimino) methyl]-6-ethoxyphenol. Journal of Molecular Structure, 2019, 1191, 129-137. (DOI: https://doi.org/10.1016/j.molstruc.2019.03.060)

18. S. Burguera, A. Frontera, and A. Bauza. Regium π Bonds Involving Nucleobases: Theoretical Study and Biological Implications. Inorganic Chemistry, 2023, 62(17), 6740-6750. (DOI: https://doi.org/10.1021/acs.inorgchem.3c00369)

19. E. Guzel, Z. Demircioğlu, C. Çiçek, and E. Agar. Experimental and theoretical approach: Local and global chemical activity, charge transfer method with DNA bases, spectroscopic, structural and electronic properties of (E)-2-(((4-fluorophenyl) imino) methyl)-4-methoxyphenol, Journal of Molecular Structure, 2020, 1204, 127451. (DOI: https://doi.org/10.1016/j.molstruc.2019.127451)

20. H.P. Frisch, R.D Hratchian, T.A. Dennington, J. Keith, A.B. Millam, A. Nielsen, J. Holder, J. Hiscocks. Gauss View, Version; Gaussian, Inc.: Wallingford, CT, USA, 2009.

21. N.M. O'boyle, A.L. Tenderholt, and K.M. Langner, Cclib: a library for package-independent computational chemistry algorithms, Journal of computational chemistry, 2008, 29(5): 839-845. (DOI: https://doi.org/10.1002/jcc.20823)

22. S. Ignatov. Moltran v. 2.5-Program for molecular visualization and thermodynamic calculations, University of Nizhny Novgorod, 2004.

23. S.R. Pilli, T. Banerjee, K. Mohanty. HOMO–LUMO energy interactions between endocrine disrupting chemicals and ionic liquids using the density functional theory: Evaluation and Comparison, Journal of Molecular Liquids, 2015, 207, 112-124. (DOI: https://doi.org/10.1016/j.molliq.2015.03.019)

24. K.B. Rai, R.R. Ghimire, C. Dhakal, K. Pudasainee, B. Siwakoti. Structural Equilibrium Configuration of Benzene and Aniline: A First-Principles Study, Journal of Nepal Chemical Society, 2024, 44(1), 1-15. (DOI: https://doi.org/10.3126/jncs.v44i1.62675)

25. H. Liu, C. Ge, G. Yu, X. Qian. Theoretical study of the structural and optical properties of cytosine analogues, Computational and Theoretical Chemistry, 2014, 1049, 75-81. (DOI: https://doi.org/10.1016/j.comptc.2014.09.026)

26. S. Limbu, T. Ojha, R.R. Ghimiri, K.B. Rai. An investigation of vibrational analysis, thermodynamics properties and electronic properties of Formaldehyde and its stretch by substituent acetone, acetyl chloride and methyl acetate using first principles analysis, Bibechana, 2024, 21(1), 23-36. (DOI: https://doi.org/10.3126/bibechana.v21i1.58684)

27. T. Ojha, S. Limbu, P.M. Shrestha, S.P. Gupta, K.B. Rai. Comparative Computational Study on Molecular Structure, Electronic and Vibrational Analysis of Vinyl Bromide based on HF and DFT Approach, Himalayan Journal of Science and Technology, 2023, 7(1), 38-49. (DOI: https://doi.org/10.3126/hijost.v7i1.61128)

28. A.S. Gidado, S. Abubakar, M.A. Shariff. DFT, RHF and MP2 based study of the thermodynamic, electronic and non-optical properties of DNA nucleobases, Bayero Journal of Pure and Applied Sciences, 2017, 10(1), 115-127. (DOI: https://doi.org/10.4314/bajopas.v10i1.17)

29. K.B. Rai, I.B. Khadka, A.R. Koirala, S.C. Ray. Insight of cleaning, doping and defective effects on the graphene surface by using methanol, Advances in Materials Research, 2021, 10(4), 283-292. (DOI: https://doi.org/10.12989/amr.2021.10.4.283)

30. W. Humphrey, A. Dalke, K. Schulten. VMD: visual molecular dynamics, Journal of Molecular Graphics, 1996, 14(1), 33-38. (DOI: https://doi.org/10.1016/0263-7855(96)00018-5)

31. J. Wiley. Introduction to solid state physics, New York, USA, 1986.

32. R.M. Martin, Electronic structure: basic theory and practical methods, Cambridge University Press, UK, 2020.

33. R. Ghimire, A.R. Magar, B. Basnet, R. Uprety, K. Pudasainee, K.B. Rai. Study of the Spectroscopic Analysis, Electronic Structure and Thermodynamic Properties of Ethyl benzene Using First-Principles Density Functional Theory, Contemporary Research: An Interdisciplinary Academic Journal, 2024, 7(1), 80-99. (DOI: https://doi.org/10.3126/craiaj.v7i1.67259)

34. J. Jerbi, M. Springborg. Computational study of the reactivity of cytosine derivatives, Journal of Computational Chemistry, 2017, 38(14), 1049-1056. (DOI: https://doi.org/10.1002/jcc.24781)

35. F. Akman, A. Demirpolat, A.S. Kazachenko, N. Issaoui, O.AI-Dossary. Molecular structure, electronic properties, reactivity (ELF, LOL, and Fukui), and NCI-RDG studies of the binary mixture of water and essential oil of pylori's Bruguieri, Molecules, 2023, 28(6), 2084. (DOI: https://doi.org/10.3390/molecules28062684)

36. A. Rana Magar, R. Ghimire, B. Baset, P.M. Shrestha, S.P. Gupta, K.B. Rai. First-principles Calculation of Cumene: Molecular Structure, Electronic Structures, Spectroscopic Analysis, and Thermodynamic Properties, Molung Educational Frontier, 2024,14(01), 1-26. (DOI: https://doi.org/10.3126/mef.v14i01.67890)

37. S. Ali, B. Lone. In AIP Conference Proceedings 2021, March, *AIP Publishing,* 2021, 2335(1).

38. S.A. Katsyuba, T.I. Burganov. Computational analysis of the vibrational spectra and structure of aqueous cytosine, Physical Chemistry Chemical Physics, 2023, 25(35), 24121-24128. (DOI: https://doi.org/10.1039/D3CP03059H)

39. K.B. Rai, N.K. Teemilsina, B. Siwakoti. First principles study of structural equilibrium configuration of Ortho-, Meta-, and Para-chloroaniline molecules, Scientific World, 2024, 17(17), 7-18. (DOI: https://doi.org/10.3126/sw.v17i17.66414)

40. V.N. Emel'yanenko, D.H. Zaitsau, E. Shoifet, F. Meurer, S.P. Verevkin, C. Schick, C. Held. Benchmark thermochemistry for biologically relevant adenine and cytosine. A combined experimental and theoretical study, The Journal of Physical Chemistry A, 2015, 119(37), 9680-9691. (DOI: https://doi.org/10.1021/acs.jpca.5b04753)

41. C. Budha, K.B. Rai. Study of the Molecular Structure, Spectroscopic Analysis, Electronic Structures and Thermodynamic Properties of Niacin Molecule Using First-principles, Journal of Nepal Chemical Society, 2024, 44(2), 1-12. (DOI: https://doi.org/10.3126/jncs.v44i2.68263)